Check for updates

Received: 5 March 2022 | Accepted: 14 August 2022

DOI: 10.1111/jopr.13595

ORIGINAL ARTICLE

ACP AMERICAN COLLEGE OF PROSTHODONTISTS Your smile. Our specialty.®

# Graphene Coated Ti-6Al-4V Exhibits Antibacterial and Antifungal Properties Against Oral Pathogens

**Xu Wang DDS** | **Weiwei Zhao DDS** | **Chen Zhao DDS** | **Wenqing Zhang MSc** | **Zhimin Yan DDS**

Department of Oral Medicine, Peking University School and Hospital of Stomatology, National Center of Stomatology, National Clinical Research Center for Oral Diseases, National Engineering Laboratory for Digital and Material Technology of Stomatology, Beijing Key Laboratory of Digital Stomatology, Research Center of Engineering and Technology for Computerized Dentistry Ministry of Health, NMPA Key Laboratory for Dental Materials, Beijing, P.R. China

**Correspondence**
Zhimin Yan, DDS, Department of Oral Medicine, Peking University School and Hospital of Stomatology, 22 South Zhongguancun Ave, Haidian District, Beijing 100081, China
Email: yzhimin96@163.com

**Funding information**
National Natural Science Foundation of China, Grant/Award Number: 81570985

## Abstract

**Purpose:** This study aimed to explore the antimicrobial properties of graphene coated Ti-6Al-4V to oral pathogens.

**Materials and methods:** Graphene directly synthesized on Ti-6Al-4V alloy was characterized by scanning electron microscopy (SEM) and Raman spectroscopy. 3-(4,5-dimethylthiazol-2-yl)-2,5-diphenyl tetrazolium bromide (MTT) assay, live/dead fluorescent staining and SEM were used to analyze the antimicrobial properties of graphene coated Ti-6Al-4V alloy to *Porphyromonas gingivalis* (*P. gingivalis*), *Fusobacterium nucleatum* (*F. nucleatum*), and *Candida albicans* (*C. albicans*). Reactive oxygen species (ROS) generation was monitored to reveal the antimicrobial mechanism.

**Results:** Graphene coated Ti-6Al-4V alloy caused a significant reduction in the presence of both bacterial and fungal pathogens as compared to uncoated Ti-6Al-4V alloy. *P. gingivalis*, *F. nucleatum*, and *C. albicans* on graphene coated Ti-6Al-4V alloy were less active than on uncoated Ti-6Al-4V alloy, and tended to become shrunk and deformed. Meanwhile, graphene coated Ti-6Al-4V alloy induced more generation of ROS in the pathogens than uncoated Ti-6Al-4V alloy.

**Conclusions:** Graphene coated Ti-6Al-4V alloy exhibited antimicrobial properties against oral pathogens, the induction of oxidative stress might be involved in its antimicrobial mechanisms.

**KEYWORDS**
Graphene, *Porphyromonas gingivalis*, *Fusobacterium nucleatum*, *Candida albicans*, Ti-6Al-4V alloy

Titanium alloys are universally used as dental implant materials.[1] It is generally accepted that titanium alloys have superior attributes such as low toxicity, good biocompatibility, excellent bone bonding capacity, and outstanding mechanical properties.[2] However, unsatisfactory antimicrobial ability is one of the disadvantages of titanium alloys.[2]

Peri-implantitis is a polymicrobial inflammatory disease, which leads to supporting bone resorption and implant loss.[3,4] Microorganisms, especially gram-negative anaerobic bacteria, such as *Porphyromonas gingivalis* (*P. gingivalis*) and *Fusobacterium nucleatum* (*F. nucleatum*) surrounding peri-implant tissue are accepted as major pathogens of peri-implantitis.[5–7] *P. gingivalis* can change the normal oral microbiota composition to one with greater pathogenicity and is considered the keystone pathogen of peri-implant inflammation, while *F. nucleatum* can connect initial and later bacterial colonizers, thereby conducive to the formation of dental plaques.[5,7]

In addition to pathogenic bacteria, *Candida albicans* (*C. albicans*) is also present in the subgingival plaque biofilm of peri-implantitis and participates in the development of peri-implant diseases.[8,9] *C. albicans* could induce co-aggregation of other microorganisms such as *F. nucleatum* and *Streptococcus gordonii* (*S. gordonii*), and contribute to the formation of multispecies biofilms on the surfaces of Ti-6Al-4V alloy, which can cause increased tissue damage of titanium-mucosal interface.[8–11]

Various methods have been explored to modify the antimicrobial performances of titanium alloys, but many shortcomings still exist. Coatings loaded with chlorhexidine

Authors Xu Wang and Weiwei Zhao contributed equally to this work.

 © 2022 by the American College of Prosthodontists. 

1532849x, 0, Downloaded from https://onlinelibrary.wiley.com/doi/10.1111/jopr.13595 by Xu Wang - Peking University , Wiley Online Library on [27/11/2022]. See the Terms and Conditions (https://onlinelibrary.wiley.com/terms-and-conditions) on Wiley Online Library for rules of use; OA articles are governed by the applicable Creative Commons License

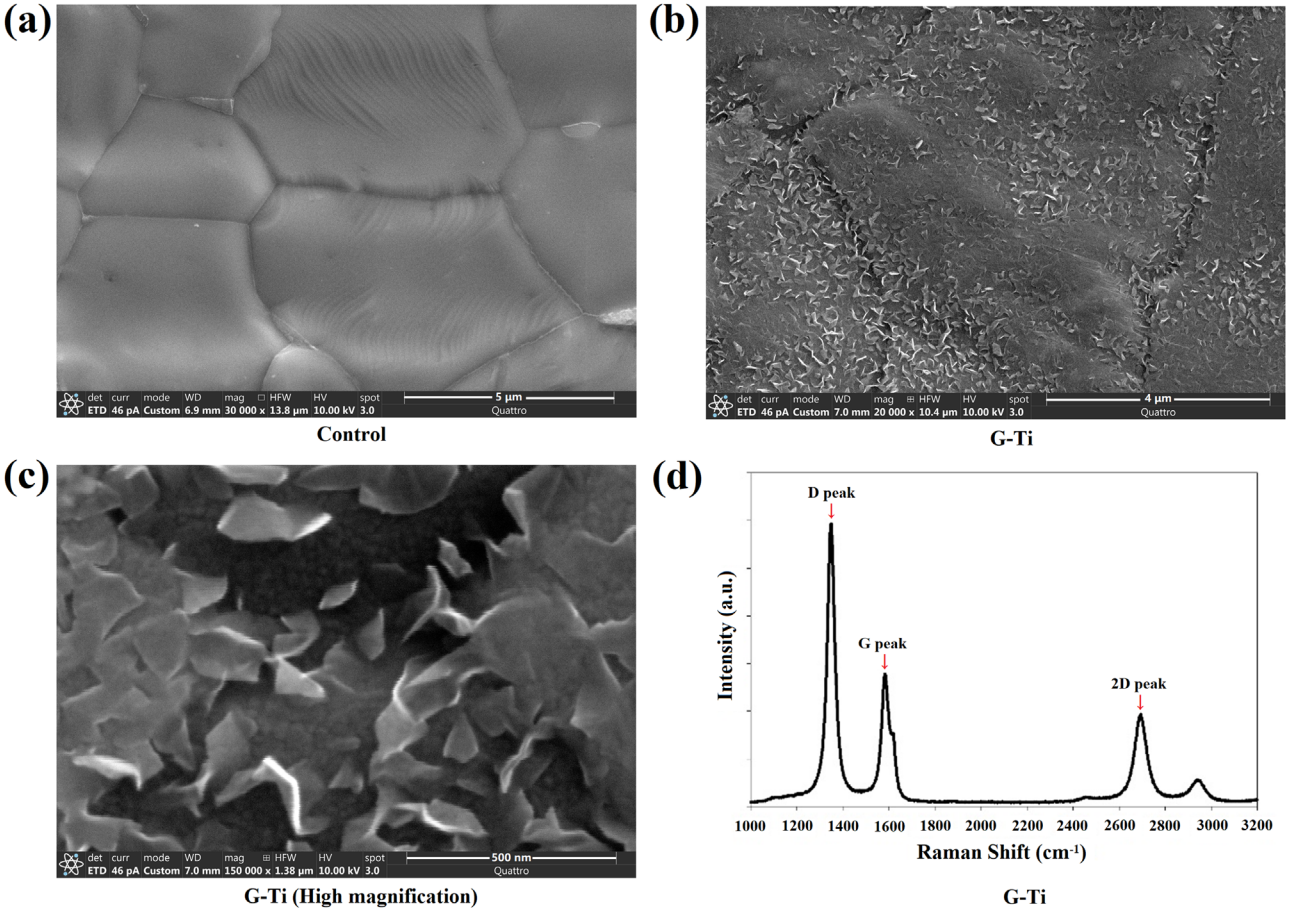


**FIGURE 1** Characterization of uncoated Ti-6Al-4V alloy (Control) and graphene coated Ti-6Al-4V alloy (G-Ti) (n = 3). (a) SEM image of Control (magnification × 30,000). (b) SEM image of G-Ti (magnification × 20,000). (c) High magnification SEM image of G-Ti (magnification × 150,000). (d) Raman spectra of G-Ti; the arrows indicate characteristic graphene peaks.

or antibiotics applied on the surface of titanium alloys only showed short-term antimicrobial efficacy and still remain controversial.[12–14] Acid etching and sand-blasting have been used to reduce the adhesion of pathogens, but might bring the risk of microcracks on the surface and decrease the fatigue properties.[15–17] Therefore, it makes sense to explore novel methods and techniques to modify the antimicrobial performances of titanium alloys, which should not impair their structural integrity and biocompatibility.

Graphene, a one-atom-thick layer of carbon atoms in a dense honeycomb two-dimensional crystal, stands out because of its lower cytotoxicity and strong antibacterial effects.[18,19] Graphene and its derivatives have been demonstrated to be promising materials as antimicrobial agents and coatings.[19] Agarwalla et al showed that the biofilm formation for *Streptococcus mutans* (*S. mutans*), *Enterococcus faecalis* (*E. faecalis*), *Pseudomonas aeruginosa* (*P. aeruginosa*), and *C. albicans* was less on graphene coated titanium than on uncoated titanium.[20] Gu et al also revealed that graphene coated titanium enhanced the antibacterial activity to *Escherichia coli* (*E. coli*) and *Streptococcus aureus* (*S. aureus*) compared to titanium substrate.[21] However, the substrates may influence the antimicrobial properties of graphene coating.[22]

Considering that few studies have explored the antimicrobial activities of graphene coating on Ti-6Al-4V alloy substrate to oral bacteria and fungi, this study mainly aimed to investigate the antimicrobial properties of graphene coated Ti-6Al-4V alloy to *P. gingivalis*, *F. nucleatum*, and *C. albicans*.

## MATERIALS AND METHODS

Graphene was donated by Dr. Feng Yu, and was synthesized on the surface of Ti-6Al-4V alloy by means of Radio Frequency Plasma Enhanced Chemical Vapor Deposition (RF-PECVD) method.[23] Briefly, the cleaned and dried Ti-6Al-4V alloy foil (thickness ≈ 100 μm) was placed at the hot center of the furnace. RF-PECVD system (13.56 MHz) was evacuated to the base pressure and heated to 500 to 700°C under a $H_2$ flow of 20 standard cubic centime per minute (sccm). Then, $H_2$ was replaced with 5 to 20 sccm $CH_4$. Growth of vertical graphene lasted for 0.5 to 2 hours. The surface morphologies of Ti-6Al-4V alloy (Control) and graphene coated Ti-6Al-4V alloy (G-Ti) were

15328849x, 0, Downloaded from https://onlinelibrary.wiley.com/doi/10.1111/jopr.13595 by Xu Wang - Peking University , Wiley Online Library on [27/11/2022]. See the Terms and Conditions (https://onlinelibrary.wiley.com/terms-and-conditions) on Wiley Online Library for rules of use; OA articles are governed by the applicable Creative Commons License

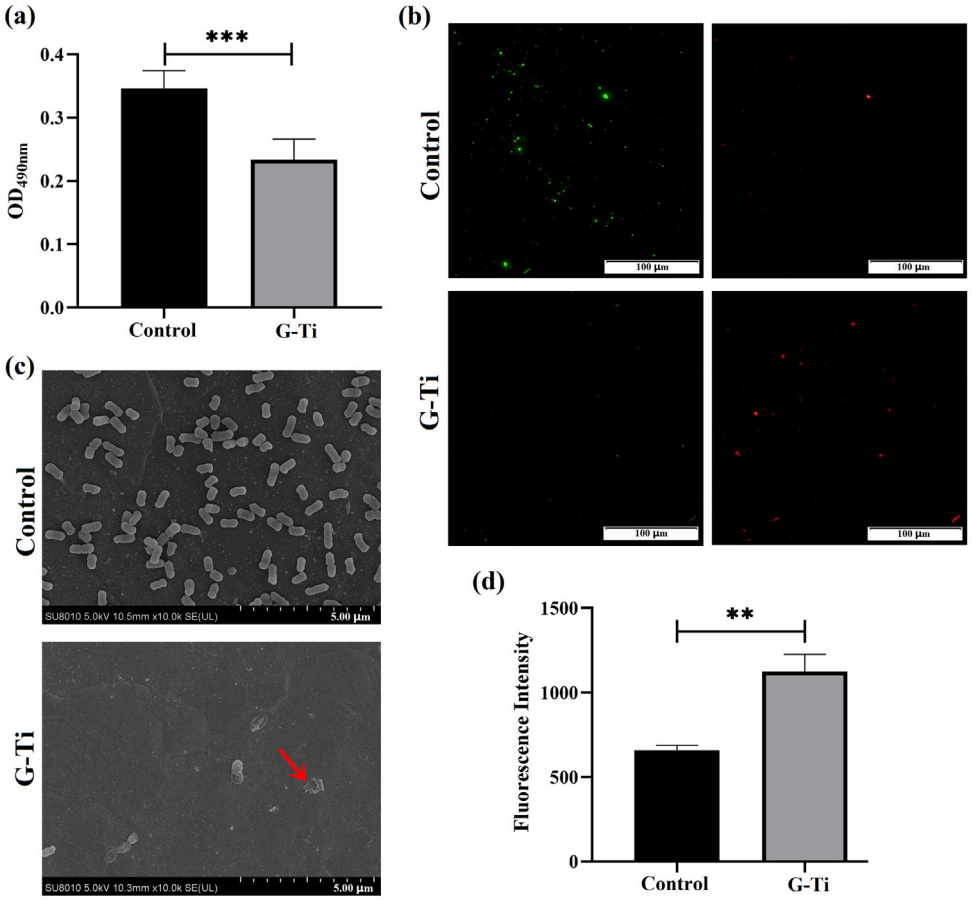


**FIGURE 2** Anti-*P. gingivalis* ability of graphene coated Ti-6Al-4V alloy. (a) Cell metabolic activities of *P. gingivalis* incubated on G-Ti or Control for 2 hours, measured by MTT assay (n = 5). (b) Live/Dead staining of *P. gingivalis* incubated on G-Ti or Control for 24 hours (n = 3), Scale bar = 100µm. (c) Representative SEM images of *P. gingivalis* incubated on G-Ti or Control for 24 hours (magnification × 10,000) (n = 3); the arrows indicate cell shrinkage and deformation. (d) Fluorescence intensity of ROS concentration in *P. gingivalis* incubated on G-Ti or Control for 12 hours (n = 3). $^{**}p < 0.01$, $^{***}p < 0.001$.

systematically characterized by scanning electron microscopy (SEM). Further, the G-Ti samples were subjected for Raman scattering spectroscopy in the air at room temperature (Raman Microscope CRM 200, Witec, Germany).

Then, uncoated Ti-6Al-4V alloy (Control) and graphene coated Ti-6Al-4V alloy (G-Ti) were mechanically cut into circular discs to fit the sizes of 24/96/-well plates (Corning, USA). Before being used for the following experiments, G-Ti were checked for the presence of graphene coating and both Control and G-Ti were sterilized at high temperature and pressure (121°C and 0.12 MPa).

*P. gingivalis* (W83) and *F. nucleatum* (ATCC25586) were grown in brain heart infusion broth (BHI broth) (Oxoid, USA) supplied with 0.0005% hemin and 0.0001% menadione at 37°C in an anaerobic system ($N_2$ 80%; $H_2$ 10%; $CO_2$ 10%), respectively. *C. albicans* (ATCC90028) was cultured in Yeast Extract Peptone Dextrose (YPD) medium (Solarbio, Beijing, China) at 37°C. All of the microorganisms were harvested at the exponential growth phase and centrifuged at 8,000 rpm for 5 minutes. Then the microorganisms were washed two times with phosphate buffered saline (PBS) (Hyclone, USA), and individually adjusted to a concentration of $10^8$ CFU/mL by measuring the optical density (OD) value. For *P. gingivalis* and *F. nucleatum*, $OD_{600}$ of 1.0 is about $10^9$ CFU/mL, while for *C. albicans*, $OD_{490}$ of 1.0 is about $2 \times 10^8$ CFU/mL.

3-(4,5-Dimethylthiazol-2-yl)-2,5-diphenyl Tetrazolium Bromide (MTT) was used to estimate the cell metabolic activities of *P. gingivalis*, *F. nucleatum*, and *C. albicans*. Fifty (50) µL of diluted microbial suspension ($10^5$-$10^6$ CFU/mL) for each microorganism was individually added into 96-well plates covered with Control or G-Ti, and incubated for 2 hours. Then, 10 µL of MTT (Solarbio, Beijing, China) was added and incubated in the dark for another 4 hours. The suspensions were collected and centrifuged at 10,000 rpm for 5 minutes, and the supernatants were discarded. The precipitate containing formazan was dissolved in 200 µL of dimethyl sulfoxide (DMSO) and the absorbance at 490 nm wavelength was measured by microtiter plate reader (BioTek, USA).

The Live/Dead BacLight Bacterial Viability Kit (Molecular Probes, USA) was used to determine the cell viabilities of microorganisms as live cells were stained with fluorescent green, while dead cells were stained with fluorescent red. Five-hundred (500) µL of diluted microbial suspension

15328849x, 0, Downloaded from https://onlinelibrary.wiley.com/doi/10.1111/jopr.13595 by Xu Wang - Peking University , Wiley Online Library on [27/11/2022]. See the Terms and Conditions (https://onlinelibrary.wiley.com/terms-and-conditions) on Wiley Online Library for rules of use; OA articles are governed by the applicable Creative Commons License

($10^5$-$10^6$ CFU/mL) for *P. gingivalis*, *F. nucleatum*, and *C. albicans* was individually incubated on the surface of Control or G-Ti in 24-well plates for 24 hours. Then the microorganisms adhering on materials were washed with PBS 3 times and immersed in 500 μL dye. After incubation in the dark at room temperature for 30 minutes, the microorganisms were observed using a confocal laser scanning microscopy (ZEISS, Jena, Germany) system or a fluorescence microscope (Olympus, Tokyo, Japan).

Scanning electron microscopy (SEM) was used to observe the morphology features of these microorganisms adhering on the surface of Control or G-Ti. Five-hundred (500) μL of diluted microbial suspension ($10^5$-$10^6$ CFU/mL) for *P. gingivalis*, *F. nucleatum*, or *C. albicans* was individually incubated on the surface of Control or G-Ti in 24-well plates for 24 hours. Then, the cells were fixed with 2.5% glutaraldehyde at 4°C for 2 hours. After that, the samples were washed 3 times with PBS and dehydrated in a gradient sequence of ethanol (25%, 50%, 75%, 90%, and 100%). Finally, they were observed by SEM (Hitachi, Tokyo, Japan).

The 2′,7′-Dichlorofluorescein diacetate assay (DCFDA) (Sigma-Aldrich, USA) was used to evaluate the reactive oxygen species (ROS) production in the microorganisms. One-hundred (100) μL of diluted microbial suspension ($10^5$-$10^6$ CFU/mL) for *P. gingivalis*, *F. nucleatum*, and *C. albicans* was individually added on the surface of Control or G-Ti in 96-well plates and incubated for 12 hours. Then, DCFDA dye (final concentration was 10 μM) was added into the 96-well plates, and incubated in the dark for 30 minutes at 37°C. The suspensions were collected and centrifugated at 10,000 rpm for 10 minutes. The precipitate was washed with PBS and resuspended into 100 μL of PBS to measure the fluorescence intensity by a Multimode Plate Reader (PerkinElmer, USA) with excitation at 488 nm and emission at 525 nm.

Unless indicated otherwise, all groups were performed in triplicates and all data were shown as mean ± standard deviation. Data were statistically assessed for normality and variance homogeneity using the Shapiro-Wilk test and F test, respectively. Two-tailed student's T-test was used to compare the difference between the two groups (GraphPad PrismR v 8.0.1.244, USA). $P < 0.05$ was regarded as statistically significant.

## RESULTS

Grains of titanium (diameter ~5 μm) were seen from the SEM image of Ti-6Al-4V alloy (Control), evidenced by titanium grain boundaries (Fig 1a). As for graphene coated Ti-6Al-4V alloy (G-Ti), horizontal graphene could be seen at smooth areas, while vertical graphene was distributed at sharp areas (Fig 1b). Graphene on Ti-6Al-4V alloy was in flakes at few hundred nanometer sizes from higher magnification SEM image of the G-Ti (Fig 1c). From typical Raman spectroscopy of graphene coating, characteristic graphene peaks at 1350cm$^{-1}$(D peak), 1600 cm$^{-1}$(G peak), and 2700 cm$^{-1}$ (2D peak) were clear (Fig 1d).

The G-Ti exhibited stronger antibacterial properties against *P. gingivalis* and *F. nucleatum* than Control. The bacterial activities of *P. gingivalis* (Fig 2a, $p = 0.0004$) and *F. nucleatum* (Fig 3a, $p = 0.0045$) in the G-Ti group were lower than in the Control group after being cultured for 2 hours. In addition, compared to the Control group, more dead bacteria of *P. gingivalis* (Fig 2b) and *F. nucleatum* (Fig 3b) could be found in the G-Ti group. As for the morphology, *P. gingivalis* (Fig 2c) and *F. nucleatum* (Fig 3c) in the Control group exhibited typically normal and plump shape, while in the G-Ti group, membrane of both bacteria was incomplete, crumpled and destroyed. Furthermore, the DCFDA assay results showed that the ROS levels of *P. gingivalis* (Fig 2d, $p = 0.0017$) and *F. nucleatum* (Fig 3d, $p = 0.0164$) were higher in the G-Ti group than in the Control group.

The G-Ti also showed greater anti-*C. albicans* property than the Control. MTT results showed that the activity of *C. albicans* in the G-Ti group was weaker than in the Control group (Fig 4a, $p = 0.0057$). A remarkable increase of dead yeast cells could be found in the G-Ti group, as compared to the Control group (Fig 4b). As shown in the SEM images, yeast cells in the G-Ti group were round and plump, while yeast cells in the Control group were shrunk and deformed (Fig 4c). What's more, the ROS level accumulated in *C. albicans* in the G-Ti group was also higher than in the Control group. (Fig 4d, $p = 0.0027$).

## DISCUSSION

Graphene and its derivatives, graphene oxide and reduced graphene oxide, are two-dimensional carbon-based materials, which possess remarkable physical, chemical, and biological properties and show great potential as dental and medical materials.[18] Herein, this study demonstrated the prominent antibacterial and antifungal properties of graphene coated Ti-6Al-4V alloy to *P. gingivalis*, *F. nucleatum* and *C. albicans*.

Previous studies have shown the antimicrobial abilities of graphene family materials to *S. mutans*, *S. aureus*, *E. coli*, and *P. gingivalis*, and explored the underlying antibacterial mechanisms.[18,19] Physically, graphene oxide was demonstrated to disrupt the membrane of *E. coli* by the sharp edges.[24] In addition, the increased hydrophobicity of graphene coating contributed to the decrease of biofilm formation for *S. mutans*, *E. faecalis*, *P. aeruginosa*, and *C. albicans*.[20] Chemically, graphene nanosheets-TiO2 coating could enhance the transfer of the electrons from bacterial membrane and lead to bactericidal actions of *E. coli* and *S. aureus*.[25] In conclusion, graphene family materials possess excellent antimicrobial properties, and the antimicrobial mechanisms may be involved in the sharp edges of the nanosheets, excellent hydrophobicity, as well as the induction of oxidative stress.

This study demonstrated the antimicrobial properties of graphene coated Ti-6Al-4V alloy to *P. gingivalis*, *F. nucleatum* and *C. albicans*. In addition, the ROS overproduction in these pathogens during culturing on graphene coated

1532849x, 0, Downloaded from https://onlinelibrary.wiley.com/doi/10.1111/jopr.13595 by Xu Wang - Peking University , Wiley Online Library on [27/11/2022]. See the Terms and Conditions (https://onlinelibrary.wiley.com/terms-and-conditions) on Wiley Online Library for rules of use; OA articles are governed by the applicable Creative Commons License

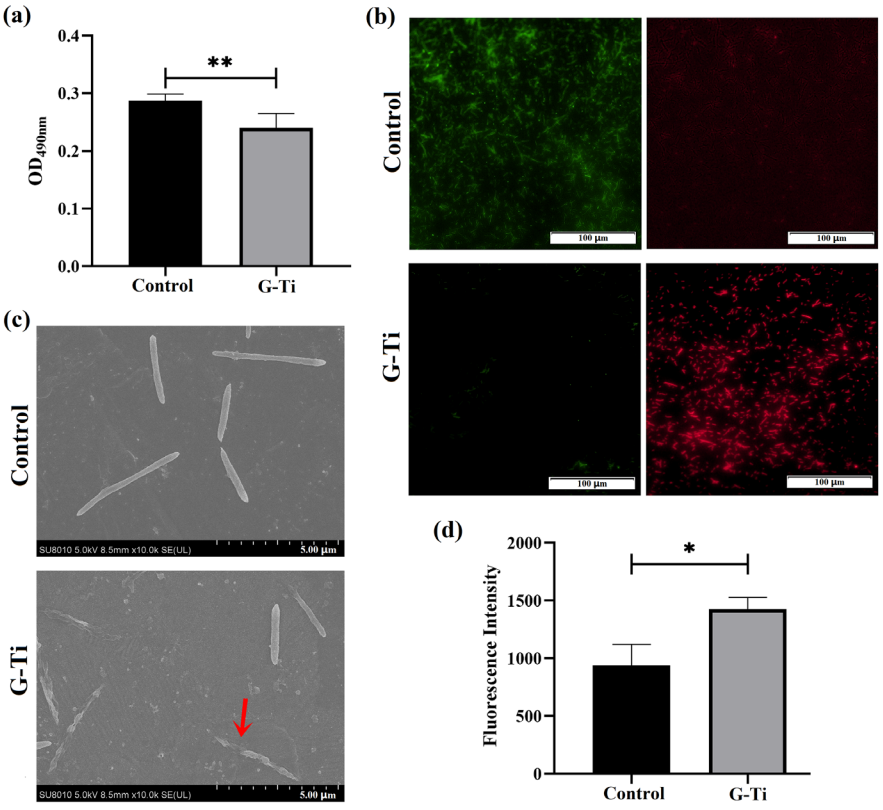


**FIGURE 3** Anti-*F. nucleatum* ability of graphene coated Ti-6Al-4V alloy. (a) Cell metabolic activities of *F. nucleatum* incubated on G-Ti or Control for 2 hours, measured by MTT assay (n = 5). (b) Live/Dead staining of *F. nucleatum* incubated on G-Ti or Control for 24 hours (n = 3), Scale bar = 100 µm. (c) Representative SEM images of *F. nucleatum* incubated on G-Ti or Control for 24 hours (magnification × 10,000) (n = 3); the arrows indicate cell shrinkage and deformation. (d) Fluorescence intensity of ROS concentration in *F. nucleatum* incubated on G-Ti or Control for 12 hours (n = 3). *$p < 0.05$, **$p < 0.01$.

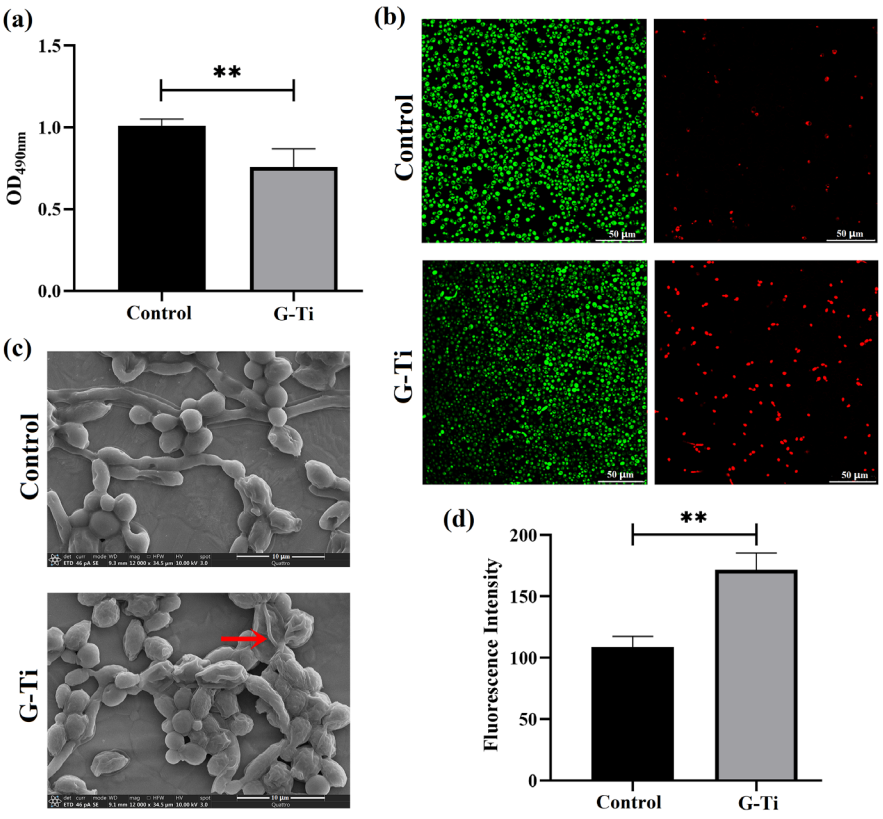


**FIGURE 4** Anti-*C. albicans* ability of graphene coated Ti-6Al-4V alloy. (a) Cell metabolic activities of *C. albicans* incubated on G-Ti or Control for 2 hours, measured by MTT assay (n = 4). (b) Live/Dead staining of *C. albicans* incubated on G-Ti or Control for 24 hours (n = 3), Scale bar = 50 µm. (c) Representative SEM images of *C. albicans* incubated on G-Ti or Control for 24 hours (magnification ×12,000) (n = 3); the arrows indicate cell shrinkage and deformation. (d) Fluorescence intensity of ROS concentration in *C. albicans* incubated on G-Ti or Control for 12 hours (n = 3). **$p < 0.01$.

1532849x, 0, Downloaded from https://onlinelibrary.wiley.com/doi/10.1111/jopr.13595 by Xu Wang - Peking University , Wiley Online Library on [27/11/2022]. See the Terms and Conditions (https://onlinelibrary.wiley.com/terms-and-conditions) on Wiley Online Library for rules of use; OA articles are governed by the applicable Creative Commons License

Ti-6Al-4V alloy might be one of the antimicrobial mechanisms. The anticorrosion properties and biocompatibility of graphene coated Ti-6Al-4V are shown in supporting information (Figure S1 and Figure S2).

*P. gingivalis* and *F. nucleatum* are major pathogens of peri-implantitis and can easily adhere to the titanium surface.[5–7] Previous research has revealed that graphene oxide nanosheets could inhibit the growth of *P. gingivalis* and *F. nucleatum*.[26] In this study, the graphene synthesized on Ti-6Al-4V alloy also showed obvious antibacterial abilities to both bacteria. In addition, Dubey et al reported that graphene could decrease the biofilm formation of *S. mutans* and *E. faecalis* on titanium.[27] That's to say, graphene could resist the growth of both gram-positive and gram-negative bacteria on titanium.

*C. albicans* is also present in the subgingival oral biofilm of patients with peri-implantitis and may participate in the development of peri-implant diseases.[8,9] Agarwalla et al revealed that graphene deposited on titanium via liquid-free technique exhibited anti-biofilm formation performance to *C. albicans*.[20] This study demonstrated this performance of graphene synthesized on Ti-6Al-4V alloy. Apart from the increased hydrophobicity of graphene films,[20] the induction of ROS observed in the present study might also be involved in the antifungal mechanisms of graphene family materials.

Various graphene family materials and/or their different substrates may possess entirely different antimicrobial properties, and the antimicrobial mechanisms may also be different. It has been reported that graphene nanosheets-$TiO_2$ coating could induce charge transfer from the bacterial membranes and enhance oxidative stress.[25] However, graphene film covering on gold substrate showed no antibacterial activity, while graphene coating on copper substrates showed bactericidal abilities because of the release of bactericidal cupric ions.[22] In this study, overproduction of ROS was observed in all of the three microorganisms when culturing on graphene coated Ti-6Al-4V alloy. ROS induction may have been partially involved in the antimicrobial mechanisms of graphene coated Ti-6Al-4V alloy, although the pathways by which ROS was induced need to be further explored.

## CONCLUSIONS

Graphene coated Ti-6Al-4V alloy exhibited greater antibacterial and antifungal properties than uncoated Ti-6Al-4V alloy. The oxidative stress may be involved in its antimicrobial mechanisms.

### ACKNOWLEDGEMENTS

We thank Dr. Feng Yu (Beijing Graphene Institute) for the kind donation of the Ti-6Al-4V alloy and graphene materials.

### CONFLICT OF INTEREST

The authors declare no potential conflict of interest.

### ORCID

*Xu Wang DDS* https://orcid.org/0000-0003-4277-041X

### REFERENCES

1. Tharani Kumar S, Prasanna Devi S, Krithika C, et al. Review of metallic biomaterials in dental applications. J Pharm Bioallied Sci 2020;12:S14-S19.
2. Silva RCS, Agrelli A, Andrade AN, et al. Titanium dental implants: an overview of applied nanobiotechnology to improve biocompatibility and prevent infections. Materials (Basel) 2022;15:3150
3. Smeets R, Henningsen A, Jung O, et al. Definition, etiology, prevention and treatment of peri-implantitis—a review. Head Face Med 2014;10:34.
4. Busscher HJ, Rinastiti M, Siswomihardjo W, et al. Biofilm formation on dental restorative and implant materials. J Dent Res 2010;89:657-665.
5. Lasserre JF, Brecx MC, Toma S. Oral microbes, biofilms and their role in periodontal and peri-implant diseases. Materials (Basel, Switzerland) 2018;11:1802
6. Carinci F, Lauritano D, Bignozzi CA, et al. A new strategy against peri-implantitis: antibacterial internal coating. Int J Mol Sci 2019;20:3897
7. de Andrade KQ, Almeida-da-Silva CLC, Coutinho-Silva R. Immunological pathways triggered by *Porphyromonas gingivalis* and *Fusobacterium nucleatum*: therapeutic possibilities. Mediators Inflamm 2019; 2019. https://doi.org/10.1155/2019/7241312
8. Alrabiah M, Alshagroud RS, Alsahhaf A, et al. Presence of *Candida* species in the subgingival oral biofilm of patients with peri-implantitis. Clin Implant Dent Relat Res 2019;21:781-785.
9. Alsahhaf A, AlâAali KA, Alshagroud RS, et al. Comparison of yeast species in the subgingival oral biofilm of individuals with type 2 diabetes and peri-implantitis and individuals with peri-implantitis without diabetes. J Periodontol 2019;90:1383-1389.
10. O'Sullivan JM, Jenkinson HF, Cannon RD. Adhesion of *Candida albicans* to oral streptococci is promoted by selective adsorption of salivary proteins to the streptococcal cell surface. Microbiology (Reading) 2000;146:41-48.
11. Souza JGS, Bertolini M, Thompson A, et al. Biofilm interactions of *Candida albicans* and mitis group *Streptococci* in a titanium-mucosal interface model. Appl Environ Microbiol 2020;86:e02950-19.
12. Garrett S, Adams DF, Bogle G, et al. The effect of locally delivered controlled-release doxycycline or scaling and root planning on periodontal maintenance patients over 9 months. J Periodontol 2000;71:22-30.
13. Pye AD, Lockhart DEA, Dawson MP, et al. A review of dental implants and infection. J Hosp Infect 2009;72(2):104-110
14. Shahid A, Aslam B, Muzammil S, et al. The prospects of antimicrobial coated medical implants. J Appl Biomater Funct Mater 2021; 19. https://doi.org/10.1177/22808000211040304
15. Pierre C, Bertrand G, Rey C, et al. Calcium phosphate coatings elaborated by the soaking process on titanium dental implants: surface preparation, processing and physical-chemical characterization. Dental materials 2019; 35(2):e25-e35
16. Kotsakis GA, Black R, Kum J, et al. Effect of implant cleaning on titanium particle dissolution and cytocompatibility. J Periodontol 2021;92:580-591.
17. Novaes Jr AB, de Souza SLS, de Barros RRM, et al. Influence of implant surfaces on osseointegration. Braz Dent J 2010;21:471-481.
18. Xie H, Cao T, RodrÃGuez-Lozano FJ, et al. Graphene for the development of the next-generation of biocomposites for dental and medical applications. Dent Mater 2017;33:765-774.
19. Nizami MZI, Takashiba S, Nishina Y. Graphene oxide: a new direction in dentistry. Appl Mater Today 2020;19:100576

1532849x, 0, Downloaded from https://onlinelibrary.wiley.com/doi/10.1111/jopr.13595 by Xu Wang - Peking University , Wiley Online Library on [27/11/2022]. See the Terms and Conditions (https://onlinelibrary.wiley.com/terms-and-conditions) on Wiley Online Library for rules of use; OA articles are governed by the applicable Creative Commons License

20. Agarwalla SV, Ellepola K, da Costa MCF, et al. Hydrophobicity of graphene as a driving force for inhibiting biofilm formation of pathogenic bacteria and fungi. Dent Mater 2019;35:403-413.
21. Gu M, Lv L, Du Fet al. Effects of thermal treatment on the adhesion strength and osteoinductive activity of single-layer graphene sheets on titanium substrates. Sci Rep 2018;8:8141.
22. Dellieu L, Lawarée E, Reckinger N, et al. Do CVD grown graphene films have antibacterial activity on metallic substrates? Carbon 2015;84:310-316
23. Yu F, Wang K, Cui L, et al. Vertical-graphene-reinforced titanium alloy bipolar plates in fuel cells. Adv Mater 2022;34:2110565
24. Lu X, Feng X, Werber JR, et al. Enhanced antibacterial activity through the controlled alignment of graphene oxide nanosheets. Proc Natl Acad Sci U S A 2017;114:E9793-E9801.
25. Yang M, Liu H, Qiu C, et al. Electron transfer correlated antibacterial activity of biocompatible graphene Nanosheets-TiO2 coatings. Carbon 2020;166:350-360
26. He J, Zhu X, Qi Z, et al. Killing dental pathogens using antibacterial graphene oxide. ACS Appl Mater Interfaces 2015;7:5605-5611.
27. Dubey N, Ellepola K, Decroix FED, et al. Graphene onto medical grade titanium: an atom-thick multimodal coating that promotes osteoblast maturation and inhibits biofilm formation from distinct species. Nanotoxicology 2018;12:274-289.

## SUPPORTING INFORMATION

Additional supporting information can be found online in the Supporting Information section at the end of this article.

**How to cite this article:** Wang X, Zhao W, Zhao C, Zhang W, Yan Z. Graphene Coated Ti-6Al-4V Exhibits Antibacterial and Antifungal Properties Against Oral Pathogens. J Prosthodont. 2022;1–7. https://doi.org/10.1111/jopr.13595

1532849x, 0, Downloaded from https://onlinelibrary.wiley.com/doi/10.1111/jopr.13595 by Xu Wang - Peking University , Wiley Online Library on [27/11/2022]. See the Terms and Conditions (https://onlinelibrary.wiley.com/terms-and-conditions) on Wiley Online Library for rules of use; OA articles are governed by the applicable Creative Commons License